Unusual Nernst Effect Suggesting Time-Reversal Violation in the Striped Cuprate Superconductor La_{2-x}Ba_{x}CuO_{4}

Lu Li, N. Alidoust, J. M. Tranquada, G. D. Gu, and N. P. Ong

Phys. Rev. Lett. **107**, 277001 — Published 27 December 2011

DOI: 10.1103/PhysRevLett.107.277001

Unusual Nernst effect suggestive of time-reversal violation in the striped cuprate $La_{2-x}Ba_xCuO_4$

Lu Li[1*], N. Alidoust[1], J. M. Tranquada[2], G. D. Gu[2], and N. P. Ong[1]
[1] *Department of Physics, Princeton University, Princeton, NJ 08544*
[2] *Brookhaven National Laboratories, Upton, NY 11973*

The striped cuprate $La_{2-x}Ba_xCuO_4$ ($x = \frac{1}{8}$) undergoes several transitions below the charge-ordering temperature $T_{co} = 54$ K. From Nernst experiments, we find that, below T_{co}, there exists a large, anomalous Nernst signal $e_{N,even}(H,T)$ that is symmetric in field H, and remains finite as $H \to 0$. The time-reversal violating signal suggests that, below T_{co}, vortices of one sign are spontaneously created to relieve interlayer phase frustration.

PACS numbers: 74.25.Dw, 74.25.Ha, 74.72.Hs

In the cuprates, there is increasing evidence that time-reversal invariance (TRI) is broken over a large portion of the phase diagram. Following a prediction in cuprates [1], signatures of TRI-violation were obtained in angle-resolved photoemission [2] and polarized neutron scattering experiments [3]. Recently, polar Kerr rotation measurements [4, 5] and polarized neutron scattering experiments [6] have uncovered firmer evidence for TRI-violating states in several cuprates.

The cuprate $La_{2-x}Ba_xCuO_4$ at doping $x \simeq \frac{1}{8}$ undergoes a remarkable series of electronic phase transitions starting at the charge-ordering temperature T_{co} (54 K) and followed by the spin-ordering temperature T_{so} (40 K) and the Berenzinski-Kosterlitz-Thouless (BKT) transition T_{BKT} (16 K) [7–10]. Below 5 K, 3D superconductivity is established. We have observed an unusual zero-field Nernst effect signal that appears below T_{co}. In principle, such a zero-field Nernst signal is forbidden in a material that has TRI. We discuss the implications of its appearance below the charge ordering temperature T_{co}.

Nernst effect measurements were carried out on $La_{2-x}Ba_xCuO_4$ crystals with $x = \frac{1}{8}$ (LBCO-$\frac{1}{8}$). We cut crystals (2, 0.7, 0.2 mm^3 along the crystal axes $\mathbf{a}, \mathbf{b}, \mathbf{c}$, respectively) from a boule and polished the faces until the normal to the broadest face was aligned with $\mathbf{c}$ to within $\pm 0.5^o$. For each curve of the Nernst signal vs. the applied field $\mathbf{H}$, we made dual measurements at two temperature gradients ($-\nabla T = 0.5$ K/mm and 0.7 K/mm) to check for linearity and reproducibility. The field was swept slowly at rates 0.2 T/min to 0.5 T/min. The measured thermal conductivity κ has a relatively weak T dependence between 10 and 60 K (varying between 6 and 7.2 W/Km). In our geometry, $-\nabla T$ is applied $||\mathbf{a}$ in the LTT phase (with axes $\hat{\mathbf{x}}||\mathbf{a}$, $\hat{\mathbf{z}}||\mathbf{c}$). With $\mathbf{H}||\hat{\mathbf{z}}$, the voltage V_y observed along $\hat{\mathbf{y}}||\mathbf{b}$ gives the observed Nernst signal, $e_y^{obs}(H,T) \equiv V_y(H,T)/(|\nabla T|d)$ with d the voltage-contact spacing (we use little "e" to denote the Nernst electric-field E_y divided by $|\nabla T|$). In Nernst experiments, e_y^{obs} is often contaminated by unavoidable pickup of the longitudinal thermopower signal caused by slight lead misalignment. We show that the anomalous signal is distinct from this pickup.

In Fig. 1, we show the observed Nernst signal at selected T from 160 K to 45 K (Panel a) and for $T \leq 35$ K (Panel b). Above 35 K, E_y is nominally linear in H with a zero-field intercept that we identify with the zero-H thermopower $S(0)$. The tilt of the curves is the conventional field-antisymmetric Nernst signal. Below the charge ordering at $T_{co} = 54$ K, however, $e_y(H,T)$ displays anomalous features which become prominent below 30 K (Panel b). The sharp, zero-field anomaly visible at 30 K grows steeply in the negative direction (relative to the zero-H value at 35 K) as T falls to 25 K. At 20 K, the anomaly assumes the shape of a narrow H-symmetric trench of full-width $\sim$2 T. As T decreases from 20 to 6 K, the trench width broadens rapidly to 15 T. At low T, we observe new structures appearing at lower fields.

Generally, the Nernst electric field E_y is antisymmetric in H, vanishing at $H = 0$. Initially, we attributed the zero-H signal in Fig. 1 to pickup of the longitudinal signal S. This assumption is valid above 60 K. However, below 54 K, a distinct field-even signal distinct from $S(H,T)$ becomes resolvable. To show this, we have measured the thermopower $S(H,T)$ simultaneously with the Nernst signal. Figure 2(a) displays the T dependence of e_y^{obs} and S measured in zero field. We find that S is positive above $T_{co} \sim 54$ K, decreases rapidly below 54 K, becoming negative below 45 K. At lower T, S attains a broad minimum at 30 K before vanishing near $T_c = 5$ K.

First, we compare the zero-H values of the observed Nernst signal $e_y^{obs}(0,T)$ (circles in Fig. 2a) and $S(0,T)$ (solid curve) over a broad interval of T. Above 54 K, the two quantities track closely. Multiplying the former by a scaling number k, we may superpose the two curves (Fig. 2a). The value of k (-9.8) implies that the voltage contacts were slightly misaligned by $\sim$130 μm along $\hat{\mathbf{x}}$. Below T_{co}, the two quantities deviate significantly. In contrast to the curve of S, $e_y^{obs}(0,T)$ oscillates vs. T, changing sign four times. With k = -9.8, we may isolate intrinsic Nernst signal $e_N(H,T)$ at finite H by substracting off the thermopower signal, viz.

$$e_N(H,T) = e_y^{obs}(H,T) - kS(H,T). \tag{1}$$

The quantity $e_N(0,T)$ in zero H, plotted in Fig. 2b, is of main interest. In the interval 30-54 K, the magnitude of $|e_N(0,T)|$ equals 0.2 μV/K, which is easily resolved in

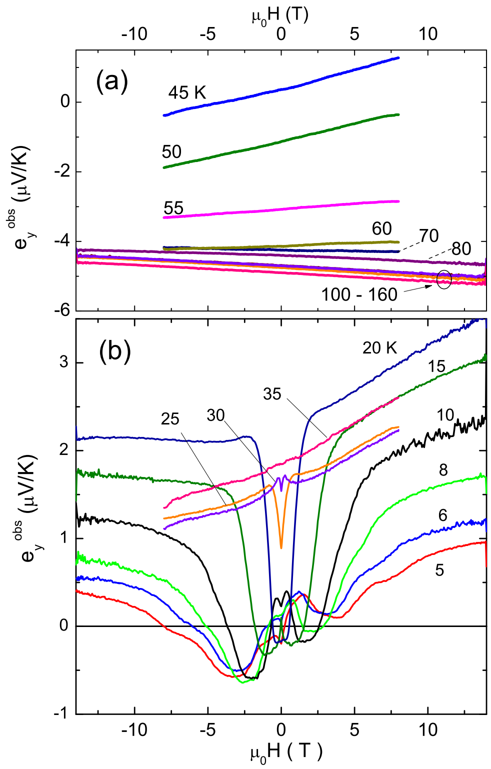

FIG. 1: (color online) Traces of the observed (raw) Nernst signal $e_y^{obs}(H,T)$ vs. applied field H at selected T from 160 to 45 K (Panel a) and below 35 K (b). The curves in Panel (a) are nominally linear in H, with an intercept at $H=0$ that comes from "pick up" of the longitudinal thermopower S due to contact misalignment. The Nernst coefficient ν is obtained from the slope near $H=0$. Below 30 K (Panel b), the curves of $e_y^{obs}(H,T)$ display prominent oscillatory features at low H which we identify with an anomalous field-symmetric Nernst signal $e_{N,even}(H,T)$.

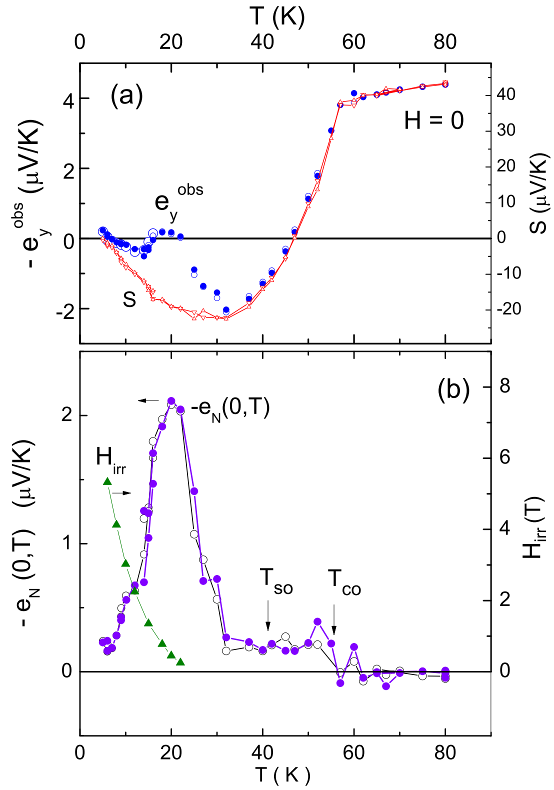

FIG. 2: (color online) Subtraction of the thermopower to extract the anomalous Nernst signal. Panel (a) compares the observed Nernst signal $E_y^{obs}(0,T)$ with the thermopower $S(0,T)$ at H=0. The Nernst results include two sets of data taken with $|\nabla T| \sim 2$ K/cm (solid symbols) and ~ 4 K/cm (open). By fixing the scaling number k= -9.8, the two curves can be superposed in the interval 50-90 K. Below 32 K, the curves strongly deviate from each other. The difference is identified with the zero-H anomalous Nernst signal $E_N(0,T)$, which is plotted in Panel (b). For 30< T < 50 K, $|E_N(0,T)|$ is small (0.2 μV/K) but well-resolved. Below 30 K, it rises abruptly to a prominent peak at 20 K before decreasing to zero near 5 K. The irreversibility field H_{irr} measured by torque magnetometry is plotted as solid triangles.

our experiment. Below 30 K, it rises steeply to a prominent maximum of 2.2 μV/K at 20 K before falling to zero near 5 K. The prominent peak, which is very sensitive to H, is the cause of the trench feature bracketing $H=0$ in the curves of e_y^{obs} vs. H plotted in Fig. 1.

It is also instructive to examine the field-symmetrized form of the observed Nernst signal $e_{y,even}^{obs}(H) = \frac{1}{2}[e_y^{obs}(H)+e_y^{obs}(-H)]$ which admixes $e_{N,even}$ and S. At 20 K, $e_{y,even}^{obs}(H,T)$ displays a deep trench centered at H=0 (Fig. 3a). As T decreases to 5 K, the trench broadens rapidly. For comparison, we also plot the curves of $S(H,T)$ (scaled by the parameter k). The features in the field profiles are clearly distinct in the two sets of curves. This difference provides strong evidence that the Nernst signal $e_N(H,T)$ has an intrinsic field-even component that is distinct from $S(H,T)$.

Subtracting $kS(H,T)$ from $e_{y,even}^{obs}(H)$ at each temperature, we isolate $e_{N,even}(H,T)$, the field-even part of the intrinsic Nernst signal in Eq. 1. The curves of $|e_{N,even}(H,T)|$ display broad peaks that shift to higher H as T decreases (Fig. 3b). The field at which the largest peak occurs is labelled $H_1(T)$. A smaller shoulder at higher field is labelled $H_2(T)$. At 20 K, the weight in $e_{N,even}(H,T)$ is concentrated in a narrow trench ($|H_1|$ ~0.5 T). As T is lowered, the two field scales H_1 and H_2 increase rapidly. They correlate with distinct features in the in-plane resistivity ρ_{ab} and the c-axis resistivity ρ_c. Below 40 K, the derivatives $d\rho_{ab}/dT$ and $d\rho_c/dT$ show maxima at the fields $H_{\rho a}(T)$ and $H_{\rho c}(T)$, respectively [7]. In Fig. 4a, we compare the T dependences of H_1 and H_2 (solid symbols) with $H_{\rho a}(T)$ and $H_{\rho c}(T)$ (open symbols) (Panel (b) shows how H_1 and H_2 are defined). As shown, H_1 equals $H_{\rho a}$ within the resolution, while H_2 is roughly of the same scale as $H_{\rho c}$. Interestingly, $H_1(T)$ follows the Debye-Waller (DW) form $H_1 = H_0\exp(-T/T_0)$, with T_0 ~6.9 K. The DW form

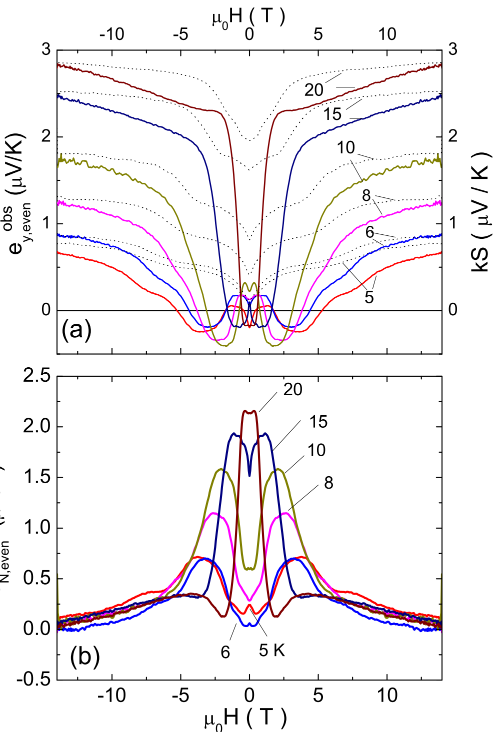

FIG. 3: (color online) Panel (a): Comparison of the raw, field-symmetrized, Nernst signal $e_{y,even}^{obs}(H,T)$ (solid curves) with the thermopower $S(H,T)$ (scaled by k = -9.8, dashed curves) at selected $T \leq 20$ K. Note that $S(H,T)$ is actually negative below 40 K (at all H shown). The two sets of curves have very different field dependences. Panel (b) displays the curves of the intrinsic field-symmetrized Nernst signal $e_{N,even}(H,T)$ obtained by subtracting the two sets of curves (see Eq. 1). The oscillatory features are absent in $S(H,T)$. At large H, $e_{N,even}(H,T)$ is suppressed to zero.

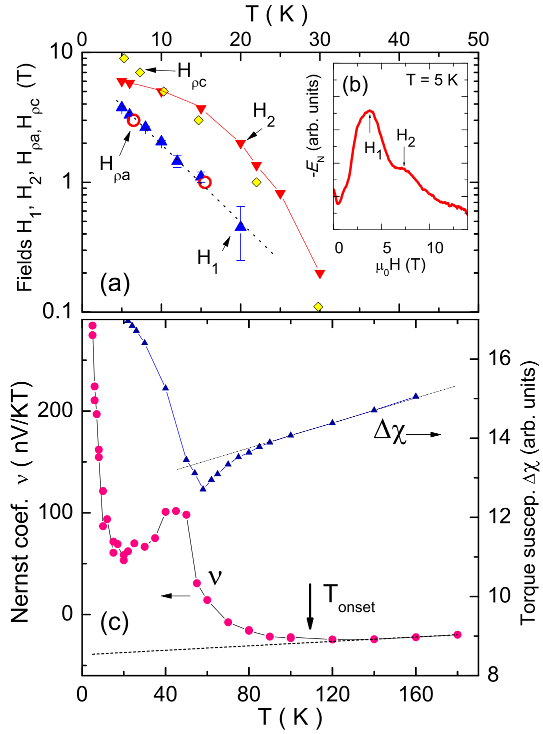

FIG. 4: (color online) Panel (a): Semilog plot of the fields $H_1(T)$, $H_2(T)$, $H_{\rho b}(T)$ and $H_{\rho c}(T)$. The data for H_1 (solid triangles) fits the form $H_0 \exp(-T/T0)$ (straight line), with H_0 = 8.28 T and T_0 = 6.86 K. $H_{\rho a}$ (open circles), inferred from $d\rho_{ab}/dT$ [7], falls on the same line as H_1. $H_{\rho c}$ (open diamonds) obtained from $d\rho_c/dT$ [7] is roughly of the same field scale as H_2. Panel (b) defines H_1 and H_2 for the curve $e_{N,even}$ at 5 K. Panel (c) displays the T dependence of the Nernst coefficient $\nu = e^{N,odd}/H$ (solid circles) and the torque susceptibility $\Delta\chi = \chi_c - \chi_a$ (solid triangles) measured with **H** (7 T) at 15° to **c**. The increase in ν below $T_{onset} \sim 110$ K correlates with a diamagnetic contribution to χ from orbital currents. Below T_{co}, the increase in ν is abruptly interrupted, but it resumes its steep increase below 20 K. Below T_{co}, the large spin susceptibility obscures supercurrent contributions to χ_c.

implies that thermally induced changes to the vortex system lead to prominent features in the anomalous Nernst signal $e_N(0,T)$. In underdoped $La_{2-x}Sr_xCuO_4$, the DW form describes the melting field of the vortex solid (with comparable T_0) [14]. We also note that the curves of S vs. H (dashed curves in Fig. 3a) display step-like increases when H exceeds $H_1 \sim H_{\rho,a}$, that match the abrupt increase in ρ_a. This pattern suggests that the collapse of the anomalous Nernst signal at H_1 leads to an increase in dissipation and entropy flow. We return to this point below.

We field-antisymmetrize the Nernst curves in Fig. 1 to obtain the conventional Nernst signal $e_{N,odd}(H) = \frac{1}{2}[e_y^{obs}(H) - e_y^{obs}(-H)]$. The Nernst coefficient, $\nu = e_{N,odd}/H$ ($H \rightarrow 0$), provides a useful comparison between field-induced vortices and the spontaneous vortices. At high T (120-180 K), ν is negative, reflecting the quasiparticle contribution to the Nernst signal (dashed line in Fig. 4b). At the onset temperature $T_{onset} \sim 110$ K, ν deviates from the dashed line and increases rapidly, as observed in $La_{2-x}Sr_xCuO_4$ (LSCO) [11]. The deviation correlates with an unusual downward deviation in the torque susceptibility $\Delta\chi = \chi_c - \chi_a$ in the torque signal (solid triangles), where χ_c (χ_a) is the susceptibility with **H**||**c** (||**a**). Above T_{co}, χ_c is $\sim 10\chi_a$ [8], so $\Delta\chi$ is dominated by χ_c. Hence the downward deviation confirms the onset of diamagnetic susceptibility in χ_c reported in Ref. [8]. (Below T_{co}, $\Delta\chi$ is complicated by a large local moment response in both χ_c and χ_a.) The magnetization results verify that, for $T > T_{co}$, the increase in ν arises from vortex fluctuations (and not from quasiparticles, as conjectured [15]). A similar agreement between Nernst and torque experiments was obtained for LSCO [11, 12]. At T_{co}, the increase in ν is abruptly interrupted. Below 20 K, however, ν resumes its steep increase as the condensate establishes long-range phase coherence.

The conventional field-antisymmetric Nernst signal shown in Fig. 4b is generated by vortices introduced by an external H. By contrast, we associate $e_{N,even}$ with vortices that are present in equilibrium at $H = 0$, as in a 2D superconductor above T_{BKT}. However, unlike the BKT problem (in which the net vorticity is zero in H=0), here we must have predominantly "up" vortices to produce a finite $e_N(0,T)$. Using torque magnetometry, we have measured the irreversibility field H_{irr} in the same crystal. As shown in Fig. 2b, H_{irr} has a very different profile from $e_N(0,T)$; $H_{irr} \to 0$ near 20 K, where $|e_N(0,T)|$ attains a maximum. Thus $e_N(0,T)$ is not caused by field-induced vortices trapped in a non-equilibrium state. (In the interval $5 < T < 20$ K, the pair condensate rigidity is strongly inhomogeneous. The vortex solid exists in isolated regions detectable by magnetization hysteresis. These regions do not contribute to the observed e_N or S.)

The results in Refs. [7, 9] have shown that pronounced superconducting fluctuations extend from T_{co} down to 5 K. The extreme anisotropy of this response indicates that the Josephson coupling between adjacent layers is highly frustrated. To explain this frustration, it has been proposed that pair-density-wave (PDW) superconductivity develops along with the stripe order [17–19]. Because the stripe modulation direction is orthogonal between adjacent layers, Josephson coupling cancels out. The abrupt interruption of the increasing trend in ν at T_{co} (Fig. 4b) is consistent with a sharp change in the character of the probed phase coherence. Below $T_{so} = 40$ K, previous results [7, 9, 20, 21], imply that competition between the PDW and uniform d-wave superconductivity exists. Eventually, at ~ 5 K, the latter dominates and true 3D long-range phase coherence prevails. The steep rise of ν below 20 K is consistent with the eventual development of uniform d-wave order.

In the PDW state, small fluctuations in the Josephson phase $\theta(\mathbf{r})$ about the uniform-phase state can lead to a gain in free energy [19]. The present results suggest to us that, below T_{co}, the sample spontaneously nucleates an array of 2D vortices in H=0, which can provide a large phase-slip of 2π. Having all the vortices be of the same sign (which breaks TRI) entails a cost in the kinetic energy of the supercurrent. However, because the local supercurrent is weak, the cost may be offset by a large gain in condensate energy provided by significant reductions in the interlayer phase frustration. Because θ is strongly fluctuating, we expect the vortices to flow freely in a gradient $-\nabla T$ and to generate a spontaneous Nernst signal.

The anomalous Nernst signal $e_N(0,T)$ attains its largest amplitude at 20 K close to T_{BKT} (16 K). Below T_{BKT}, the small but finite ρ_{ab} implies that phase rigidity extends in the a-b plane over sizeable lengths at H=0 [7]. However, when H exceeds $H_{\rho a}$, the collapse of the rigidity produces an increase in ρ_{ab}. As mentioned, this coincides with a steep increase in S which measures entropy flow (Fig. 3a), as well as the collapse of $e_{N,even}$ above H_1 (Fig. 3b). This suggests to us that the spontaneous vortices, when present, help to establish a phase-coherent state that has low dissipation and low entropy. At the larger field $H_{\rho c}$, the step increase in ρ_c signals the loss of interlayer coherence. This is also reflected in $e_{N,even}$ as H_2, but as a much weaker feature.

Despite the spontaneous nature of the time-reversal violation, some external influence must nudge the system into selecting one direction in a given experiment. We tried to change the sign by warming the sample to 290 K and then cooling in a different superconducting magnet, but it remained the same. We also tried field-cooling in $H = 14$ T from 290 K, and also swept the field between +14 and -14 T both above and below T_{co} but could not alter the sign. A. Kapitulnik has suggested to us that a weak magnetic ordering may onset at 360 K. Field-cooling from above 360 K may pre-select the sign; this is left for a future investigation.

Recently, we learned of polar-Kerr rotation TRI violating results in LBCO-$\frac{1}{8}$ [22]. The Kerr angle θ_K in $H = 0$ is unresolved from zero above T_{co}, but increases abruptly at T_{co}, reaching a sharp maximum at 41 K.

We acknowledge valuable discussions with S. A. Kivelson, E. Fradkin, E. Berg and A. Kapitulnik. We are indebted to Kivelson for valuable insights, and Kapitulnik for sharing unpublished Kerr results and suggestions. The research is supported at Princeton by the U.S. National Science Foundation (Grant DMR 0819860), and at BNL by the Office of Basic Energy Sciences, U.S. Department of Energy (Contract No. DE-AC02-98CH10886).

* *Present address of LL: Department of Physics, Univ. Michigan, Ann Arbor, MI*

[1] C. M. Varma, Phys. Rev. B **55**, 14554 (1997); Phys. Rev. Lett. **83**, 3538 (1999).
[2] A. Kaminski *et al.*, Nature (London) **416**, 610 (2002).
[3] Fauque, Y. Sidis, V. Hinkov, S. Pailhes, C. T. Lin, X. Chaud, and P. Bourges, Phys. Rev. Lett. **96**, 197001 (2006); A. Mook, Y. Sidis, B. Fauque, V. Baledent, and P. Bourges, Phys. Rev. B **78**, 020506 (2008).
[4] Jing Xia *et al.*, Phys. Rev. Lett. **100**, 127002 (2008).
[5] R.H. He *et al.*, Science **331**, 1579 (2011).
[6] Y. Li, V. Baledent, N. Barisic, Y. Cho, B. Fauque, Y. Sidis, G. Yu, X. Zhao, P. Bourges, and M. Greven, Nature (London) **455**, 372 (2008).
[7] Q. Li, M. Hücker, G. D. Gu, A. M. Tsvelik, and J. M. Tranquada, Phys. Rev. Lett. **99**, 067001 (2007).
[8] M. Hücker, G. D. Gu, and J. M. Tranquada, Phys. Rev. B **78**, 214507 (2008).
[9] J. M. Tranquada, G. D. Gu, M. Hücker, Q. Jie, H.-J. Kang, R. Klingeler, Q. Li,1 N. Tristan, J. S. Wen, G. Y. Xu, Z. J. Xu, J. Zhou, and M. v. Zimmermann, Phys. Rev. B **78**, 174529 (2008).
[10] M. Hücker, M. v. Zimmermann, G. D. Gu, Z. J. Xu, J. S. Wen, Guangyong Xu, H. J. Kang, A. Zheludev, and J.

M. Tranquada, Phys. Rev. B **83**, 104506 (2011).
[11] Yayu Wang, Lu Li, and N. P. Ong, Phys. Rev. B **73**, 024510 (2006).
[12] Lu Li, *et al.*, Phys. Rev. B **81**, 054500 (2009).
[13] Yayu Wang, Lu Li, M. J. Naughton, G. Gu, S. Uchida and N. P. Ong, Phys. Rev. Lett. **95**, 247002 (2005).
[14] Lu Li, J. G. Checkelsky, Seiki Komiya, Yoichi Ando and N. P. Ong, Nature Physics **3**, 311 (2007).
[15] Olivier Cyr-Choiniere *et al.*, Nature, **458**, 743 (2009).
[16] Yayu Wang, N. P. Ong, Z.A. Xu, T. Kakeshita, S. Uchida, D. A. Bonn, R. Liang and W. N. Hardy, Phys. Rev. Lett. **88**, 257003 (2002).
[17] E. Berg, E. Fradkin, E.-A. Kim, S. A. Kivelson, V. Oganesyan, J. M. Tranquada and S. C. Zhang, Phys. Rev. Lett. **99**, 127003 (2007).
[18] A. Himeda, T. Kato, and M. Ogata, Phys. Rev. Lett. 88, 117001 (2002).
[19] E. Berg, *et al.*, Nature Phys. **5**, 830 (2009); E. Berg *et al.*, New J. Phys. **11**, 115004 (2009).
[20] T. Valla, A. V. Federov, J. Lee, J. C. Davis, and G. D. Gu, Science **314**, 1914 (2006).
[21] R.-H. He *et al.*, Nat. Phys. **5**, 119 (2009).
[22] A. Kapitulnik, *private communication*.